JPET Fast Forward. Published on August 7, 2013 as DOI: 10.1124/jpet.113.207621
This article has not been copyedited and formatted. The final version may differ from this version.

Title Page

OLANZAPINE ACTIVATES HEPATIC MAMMALIAN TARGET OF RAPAMYCIN (mTOR): NEW MECHANISTIC INSIGHT INTO METABOLIC DYSREGULATION WITH ATYPICAL ANTIPSYCHOTIC DRUGS*

Robin H. Schmidt, Jenny D. Jokinen, Veronica L. Massey, K. Cameron Falkner, Xue Shi, Xinmin Yin, Xiang Zhang, Juliane I. Beier, and Gavin E. Arteel

Department of Pharmacology and Toxicology, University of Louisville Health Sciences Center, Louisville, KY 40292, USA (RHS, JDJ, VLM, JIB, GEA)

Department of Medicine, University of Louisville Health Sciences Center, Louisville, KY 40292, USA (KCF)

Department of Chemistry, University of Louisville, Louisville, KY 40292, USA (XS, XY, XZ)

JPET Fast Forward. Published on August 7, 2013 as DOI: 10.1124/jpet.113.207621
This article has not been copyedited and formatted. The final version may differ from this version.

Running title: Olanzapine and hepatic metabolic dysfunction

Contact information: Gavin E. Arteel, Ph.D.
Department of Pharmacology and Toxicology
University of Louisville Health Sciences Center
Louisville, KY, 40292
Phone#: (502) 852-5157
FAX#: (502) 852-3242
e-mail: gavin.arteel@louisville.edu

text pages: 27
number of tables: 1
number of figures: 6
number of references: 49
word count: Abstract, 247; Introduction, 464; Discussion, 938

Abbreviations: 4EBP1, eukaryotic translation initiation factor 4E binding protein 1; *Acly*, ATP citrate lyase; Akt, protein kinase B; ALT, alanine aminotransferase; AMPK, AMP-activated protein kinase; AST, aspartate aminotransferase; CNS, central nervous system; *Cpt1a*, carnitine palmitoyltransferase 1a; DEXA, dual-energy x-ray absorptiometry; *Fasn*, fatty acid synthase; FCCP, Carbonyl cyanide 4-(trifluoromethoxy)phenylhydrazone; GCxGC-TOF MS, comprehensive two-dimensional gas chromatography time-of-flight mass spectrometry; *Gck*, glucokinase; *Glut1*, glucose transporter type 1; *Glut4*, glucose transporter type 4; *Gsk3b*, glycogen synthase kinase-3β; H&E, hematoxylin and eosin; HDL, high-density lipoprotein; LDL, low-density lipoprotein; MTBSTFA, N-(tert-butyldimethylsilyl)-N-methyltrifluoroacetamide; mTOR, mammalian target of rapamycin; NEFA, non-esterified fatty acids; OCR, oxygen consumption rate; OGTT, oral glucose tolerance test; OLZ, olanzapine; p70S6K, 70 kDa ribosomal protein S6 kinase; *Pck1*, phosphoenolpyruvate carboxykinase 1; PAS, periodic acid-Schiff; PPR, proton production rate; *Srebf1*, sterol regulatory element-binding protein 1; TBDMSCI, tert-butyldimethylchlorosilane; TG, triglycerides; VLDL, very-low density lipoprotein.

Section assignment: Gastrointestinal, hepatic, pulmonary and renal.

Abstract

Olanzapine (OLZ) is an effective treatment for schizophrenia and other disorders, but causes weight gain and metabolic syndrome. Most studies to date have focused on potential effects of OLZ on CNS mediation of weight; however, peripheral changes in liver or other key metabolic organs may also play a role in systemic effects of OLZ. The purpose of this study was to therefore investigate the effects of OLZ on hepatic metabolism in a mouse model of OLZ exposure. Female C57Bl/6J mice were administered OLZ (8 mg/kg/d) or vehicle subcutaneously by osmotic minipumps for 28 days. Liver and plasma were taken at sacrifice for biochemical analyses and for GCxGC-TOF MS metabolomics analysis. OLZ increased body weight, fat pad mass, and liver-to-body weight ratio without commensurate increase in food consumption, indicating that OLZ altered energy expenditure. Expression and biochemical analyses indicated that OLZ induced anaerobic glycolysis and caused a 'pseudo-fasted' state, which depleted hepatic glycogen reserves; OLZ caused similar effects in cultured HepG2 cells, as determined by Seahorse analysis. Metabolomic analysis indicated that OLZ increased hepatic concentrations of amino acids that can alter metabolism via the mTOR pathway; indeed, hepatic mTOR signaling was robustly increased by OLZ. Interestingly, OLZ concomitantly activated AMPK signaling. Taken together, these data suggest that disturbances in glucose and lipid metabolism caused by OLZ in liver may be mediated, at least in part, via simultaneous activation of both catabolic (AMPK) and anabolic (mTOR) pathways, and yield new insight into the metabolic side effects of this drug.

JPET Fast Forward. Published on August 7, 2013 as DOI: 10.1124/jpet.113.207621
This article has not been copyedited and formatted. The final version may differ from this version.

Introduction

Olanzapine (OLZ) is one of the most effective drug options for managing the symptoms of schizophrenia and bipolar disorder (Lee, et al., 2002). Unlike the first-generation antipsychotic medications (e.g., haloperidol), the risk of tardive dyskinesia is low with OLZ, and acute idiosyncratic toxicity is rare. These attributes make OLZ a drug of choice to treat severe mental illness. Indeed, the lack of severe side effects has expanded the off-label use of the drug for indications such as dementia and treatment-resistant anxiety disorders (Maher and Theodore, 2012). Although OLZ does not share the severe toxicity of its first-generation predecessors, it does have side effects that limit its therapeutic potential. Numerous studies show that OLZ causes substantial weight gain only weeks after the start of administration, and that this weight gain persists throughout treatment (Mathews and Muzina, 2007); these effects strongly negatively influence patient treatment compliance (Weiden, et al., 2004).

OLZ-induced weight gain is not only an issue for patient compliance, but can also induce sequelae associated with weight gain/obesity, such as glucose intolerance and/or insulin resistance. Interestingly, the changes induced by OLZ administration in carbohydrate and lipid metabolism may in fact precede weight gain, which suggests a potential direct effect of the drug on these pathways (Chintoh, et al., 2008). The side effects of OLZ on weight gain and glucose metabolism are particularly relevant at this time, with obesity increasing at an alarming rate in the US and other industrialized countries (Ogden, et al., 2006). Moreover, even within an increasingly overweight general population, obesity disproportionately affects individuals with severe mental illnesses (Allison, et al., 2009). It is therefore necessary to develop strategies that prevent, minimize, or reverse the adverse metabolic effects that occur during OLZ treatment, especially for a population already at risk for obesity and its sequelae (Heiskanen, et al., 2003).

The beneficial effects of OLZ are assumed to be mediated at the level of the central nervous system (CNS). Not surprisingly, most studies into the metabolic side effects of OLZ have also focused on the CNS (Weston-Green, et al., 2012). Although the CNS clearly plays a key role in regulating food consumption, obesity, dyslipidemia and diabetes (Sandoval, et al., 2009;Grayson, et al., 2013), peripheral organs also significantly contribute to metabolic dysregulation in the intact organism. To date, very little is understood about the potential effects of OLZ administration on peripheral organs critical for metabolic homeostasis. The liver is key for overall glucose and lipid homeostasis and recent studies have suggested that the effect of OLZ on the liver may contribute to its metabolic disturbances (Girault, et al., 2012). The purpose of the current study was therefore to explore the effects of OLZ on indices of carbohydrate and lipid metabolism in this organ and to determine underlying mechanisms in a mouse model of OLZ exposure.

JPET Fast Forward. Published on August 7, 2013 as DOI: 10.1124/jpet.113.207621
This article has not been copyedited and formatted. The final version may differ from this version.

Materials and Methods

Animals and treatments

Female C57BL/6J mice (8 weeks old) were purchased from The Jackson Laboratory (Bar Harbor, ME). Mice were housed in a pathogen-free barrier facility accredited by the Association for Assessment and Accreditation of Laboratory Animal Care, and procedures were approved by the University of Louisville Institutional Animal Care and Use Committee. Food and tap water were allowed ad libitum. One week prior to the initiation of the experiment, animals were switched from standard chow to purified TD.08485 diet (Harlan Laboratories, Madison, WI) to avoid any batch-to-batch variability in the food content (see Figure 1A). Olanzapine [8 mg/kg/d; (Kapur, et al., 2003)] or vehicle (saline) was given s.c. via osmotic minipumps (Alzet, Cupertino, CA) for 28 days. To avoid concerns of OLZ degradation, pumps were replaced after two weeks (van der Zwaal, et al., 2008). Animals were weighed on a weekly basis and food consumption was recorded twice per week. After 28 days, the mice were anesthetized with ketamine/xylazine (100/15 mg/kg i.p.) and minipumps were removed. Body composition was assessed by dual-energy x-ray absorptiometry (DEXA) using a Lunar PIXImus densitometer (Lunar Corp., Madison, WI), according to manufacturer's instructions. Blood was collected from the vena cava just prior to sacrifice by exsanguination, and citrated plasma was stored at −80 °C for further analysis. Portions of liver tissue were frozen immediately in liquid nitrogen, fixed in 10% neutral buffered formalin, or frozen-fixed for subsequent sectioning and mounting on microscope slides. Blood, liver, and gonadal fat pads were collected for later analysis.

Oral glucose tolerance test (OGTT)

Oral glucose tolerance (Andrikopoulos, et al., 2008) was evaluated at 25 days of OLZ exposure. Briefly mice were transferred to cages that had been cleared of food and bedding and fasted for 6 hours. Blood was sampled from the tail vein immediately after the fasting period, and then 15, 30, 60, 90 and 120 minutes after oral administration of 2 mg/kg D-(+)-glucose (Sigma, St. Louis,

MO) in sterile saline (4 ml/kg) solution. Glucose concentrations were measured using an Accu-Chek® Aviva Plus glucometer and test strips (Roche Diagnostics Corp., Indianapolis, IN).

Biochemical analyses and histology

Plasma levels of alanine aminotransferase (ALT), aspartate aminotransferase (AST), total cholesterol, HDL, LDL, VLDL, triglycerides (TG), and glucose were determined by the Piccolo® Lipid Panel Plus Reagent Disc, used with the Piccolo xpress™ Chemistry Analyzer (Abaxis, Inc., Union City, CA), according to manufacturer's instructions. Paraffin-embedded sections of liver were stained with hematoxylin and eosin (H&E) to assess overall hepatic structure. Hepatic lipids (TG and NEFA – non-esterified fatty acids) were extracted in chloroform:methanol (Bligh and Dyer, 1959) and measured as described previously (Bergheim, et al., 2006). Results were normalized to wet weight of extracted tissue. For detection of hepatic neutral lipids in tissue, 10 μm frozen sections were stained with Oil Red O (Sigma Chemical Co., St. Louis, MO) for 10 min., washed, and counterstained with hematoxylin for 45 seconds (Bergheim, et al., 2006). For hepatic glycogen staining, paraffin sections (5 μm) were deparaffinized and rehydrated, oxidized in 0.5% periodic acid solution for 5 min., washed, placed in Schiff reagent for 15 min., washed, and counter-stained with hematoxylin for 1 min. Staining was quantitated by image analysis, as described previously (Bergheim, et al., 2006).

RNA isolation and real-time RT-PCR.

RNA extraction and real-time RT-PCR was performed as described previously (Bergheim, et al., 2006). The PCR primers and probes were purchased premade from Applied Biosystems (Carlsbad, CA) and designed to span introns to avoid amplification of any contaminating DNA. The comparative C_T method was used to determine fold differences between samples and the calibrator gene (β-actin) and purity of PCR products was verified by gel electrophoresis. The

JPET Fast Forward. Published on August 7, 2013 as DOI: 10.1124/jpet.113.207621
This article has not been copyedited and formatted. The final version may differ from this version.

comparative C_T method determines the amount of target, normalized to an endogenous reference (β-actin) and relative to a calibrator ($2^{\Delta\Delta Ct}$).

Immunoblots.

Frozen liver samples were homogenized in RIPA buffer (20 mM Tris pH 7.4, 150 mM NaCl, 1 mM EDTA, 1 mM EGTA, 1 mM β-glycerophosphate, 1 mM Na_3VO_4, and 1% w/w Triton X-100) containing protease, tyrosine/phosphatase, and serine/threonine phosphatase inhibitor cocktails (Sigma, St. Louis, MO). Lysates were sonicated and subsequently centrifuged for 5 min. at 16,000×g. Protein concentration of the supernatants was determined with the Bio-Rad DC Protein Assay (Bio-Rad, Hercules, CA, USA); 100 µg of total protein were mixed with 4× sample loading buffer (250 mM Tris pH 7.4, 10% SDS, 20% 2-mercaptoethanol, 40% glycerol and 0.01% w/v bromophenol blue) and incubated at 95 °C for 5 min. Samples were loaded onto SDS–polyacrylamide gels (Bio-Rad Laboratories, Hercules, CA), followed by electrophoresis and Western blotting onto PVDF membranes (Hybond P, Amersham Biosciences, Piscataway, NJ, USA). Antibodies against p-AMPKα, AMPKα, p-Akt, Akt, p-mTOR, mTOR, p-p70S6K, p-4EBP1 (Cell Signaling, Danvers, MA, USA) and p70S6K and 4EBP1 (Bethyl Laboratories, Montgomery, TX) were used at the dilutions recommended by the suppliers. Horseradish peroxidase-coupled secondary antibodies and chemiluminescence detection reagents were from Pierce (Rockford, IL, USA). The signals were detected employing Classic Blue™ autoradiography film BX (MIDSCI, St. Louis, MO). Densitometric quantitation was performed with UN-SCAN IT analysis software (Silk Scientific, Orem, UT), as described previously (Bergheim, et al., 2006).

Bioenergetic measurements (HepG2 cells)

Bioenergetic measurements were made using an XF96 Extracellular Flux Analyzer (Seahorse Biosciences, Billerica, MA). HepG2 cells (American Type Culture Collection, Manassas, VA)

JPET Fast Forward. Published on August 7, 2013 as DOI: 10.1124/jpet.113.207621
This article has not been copyedited and formatted. The final version may differ from this version.

were plated at 10,000 cells per well and grown for 24 h in DMEM (Gibco, Carlsbad, CA) containing either glucose (25 mM) or galactose (10 mM) and 6 mM pyruvate. Immortalized cells preferentially use anaerobic glycolysis to meet energy demands, even in the presence of adequate oxygen (Warburg, et al., 1967). Anaerobic glycolysis of galactose yields no net ATP, and forces cells to rely on oxidative phosphorylation (Marroquin, et al., 2007). Cells were then treated with graded concentrations of olanzapine from 0–25 μM. One hour prior to the commencement of measurements the media was changed to unbuffered DMEM (Seahorse Biosciences) containing the same concentrations of sugars, pyruvate or olanzapine. The XF96 Extracellular Flux analyzer measures OCR (oxygen consumption rate) and PPR (proton production rate) in a small transient chamber in specialized plates. Seeding density was optimized under the cell culture conditions described to ensure linear oxygen consumption and adequate mixing during the re-equilibration phases. Coupled and uncoupled OCR and PPR measurements were made by addition of oligomycin (1 μg/mL) and carbonyl cyanide 4-(trifluoromethoxy)phenylhydrazone (FCCP; 1 μM), respectively, through sequential injections from ports in the Seahorse Flux Pak cartridges.

Metabolite sample preparation

A sample of liver tissue was weighed and homogenized for 2 min after adding water at a ratio of 100 mg liver tissue/mL water. The homogenized sample was then stored at –80 °C until use. A 100 μL aliquot of the homogenized liver sample and 400 μL ice cold methanol were mixed and vortexed for 2 min, then incubated for 10 min on ice followed by another 2 min vortex. The mixtures were centrifuged at 4 °C for 10 min at 15000 G. 400 μL of the supernatant was aspirated into a micro centrifuge tube and dried in a centrifugal evaporator (SpeedVac, Thermo-Fisher, Waltham, MA) overnight. The extracted metabolites were then dissolved in 40 μL acetonitrile. After adding 40 μL N-(tert-butyldimethylsilyl)-N-methyltrifluoroacetamide (MTBSTFA) mixed with 1% tert-butyldimethylchlorosilane (TBDMSCI), the mixture was

sonicated for 3 hours followed by overnight derivatization at room temperature. The samples were then transferred to GC vials for analysis. The derivatization was performed just prior to GC×GC–TOF MS analysis.

GC×GC –TOF MS analysis

The LECO Pegasus 4D GC×GC –TOF MS instrument was equipped with an Agilent 6890 gas chromatograph and a Gerstel MPS2 auto-sampler (GERSTEL Inc., Linthicum, MD), featuring a LECO two-stage cryogenic modulator and secondary oven. The primary column was a 60 m × 0.25 mm $^{1}d_{c}$ × 0.25 µm $^{1}d_{f}$, DB-5ms GC capillary column (phenyl arylene polymer virtually equivalent to a (5%-phenyl)-methylpolysiloxane). A second GC column of 1 m × 0.25 mm $^{1}d_{c}$ × 0.25 µm $^{2}d_{f}$, DB17ms [(50% phenyl)-methylpolysiloxane)] was placed inside the secondary GC oven after the thermal modulator. Both columns were obtained from Agilent Technologies (Agilent Technologies J&W, Santa Clara, CA). The helium carrier gas (99.999% purity) flow rate was set to 2.0 mL/min at a corrected constant flow via pressure ramps. The inlet temperature was set at 280 °C. The primary column temperature was programmed with an initial temperature of 60 °C for 0.5 min and then ramped at 5 °C/min to 270 °C and kept for 15 min. The secondary column temperature program was set to an initial temperature of 70 °C for 0.5 min and then also ramped at the same temperature gradient employed in the first column to 280 °C accordingly. The thermal modulator was set to +15 °C relative to the primary oven, and a modulation time of P_M = 2 s was used. The mass range was set as 29−800 *m/z* with an acquisition rate of 200 mass spectra per second. The ion source chamber was set at 230 °C with the transfer line temperature set to 280 °C, and the detector voltage was 1450 V with electron energy of 70 eV. The acceleration voltage was turned on after a solvent delay of 674 s. The split ratio was set at 25:1.

GC×GC–TOF MS data analysis:

JPET Fast Forward. Published on August 7, 2013 as DOI: 10.1124/jpet.113.207621
This article has not been copyedited and formatted. The final version may differ from this version.

The GC×GC–TOF MS data were processed using LECO's instrument control software (ChromaTOF) for peak picking and tentative metabolite identification, followed by retention index matching, peak merging, peak list alignment, normalization, and statistical significance test using MetPP software (Wei, et al., 2013). For metabolite identification using ChromaTOF, each chromatographic peak was tentatively assigned to a metabolite if its experimental mass spectrum and a database spectrum have a spectral similarity score no less than 600. The retention index matching in MetPP was performed using the iMatch method with the *p*-value threshold set as $p \leq 0.001$ (Zhang, et al., 2011). The pairwise two-tail *t*-test was used to determine whether a metabolite has a significance abundance difference between sample groups by setting the threshold of false discovery rate $q \leq 0.3$. Functional clustering, enrichment and pathway analysis of the regulated metabolites was carried out using Metacore (Thomson Reuters, http://www.genego.com/metacore.php) platform, according to the site's instructions. Through this platform, metabolites were analyzed using the map folders, pathway maps, process networks and metabolic networks enrichment analysis. Final networks were transferred to Pathway Map Creator tool (Thomson Reuters) to create a signaling map.

Statistical analyses.

Results are reported as means±SEM (n=4-8). T-test or repeated measures ANOVA was used for the determination of statistical significance between control and OLZ groups, as appropriate. A *p* value less than 0.05 was selected before the study as the level of significance.

JPET Fast Forward. Published on August 7, 2013 as DOI: 10.1124/jpet.113.207621
This article has not been copyedited and formatted. The final version may differ from this version.

RESULTS

OLZ administration increases weight and adiposity

Average body weight at the beginning of the study was 19.4 ± 0.1 g, and did not significantly differ between the groups. All animals gained weight during the course of the study and there was no mortality or morbidity in any group. OLZ administration did not significantly increase food consumption compared to animals administered vehicle ("control"). Despite no apparent increase in food consumption, OLZ administration significantly increased body weight gain by ~40% over controls (panel B), similar to what has been observed previously by other groups (Cope, et al., 2005). An increase in body fat percentage and gonadal fat pad mass accompanied the weight gain (panel C and representative pictures, panel D) in OLZ-exposed animals.

OLZ promotes hepatic lipid accumulation

Obesity and/or metabolic syndrome commonly cause lipids to accumulate in the liver (i.e., steatosis). As OLZ administration increased body weight and total body fat (Figure 1), the effect of OLZ on hepatic lipid accumulation was determined. A crude index of hepatic lipid accumulation is liver size. OLZ increased liver weight as indicated by the elevation in liver weight to body weight ratio (Figure 2, panel C). Four weeks of OLZ treatment also increased hepatic fat, as indicated by the presence of macro- and micro-vesicular lipid droplets in hematoxylin and eosin staining (Figure 2, panel A, top). This effect of OLZ on hepatic lipid accumulation was confirmed by Oil Red O staining (Figure 2, panel A, bottom). OLZ administration significantly elevated hepatic TG content ~2-fold; interestingly, this increase in TG was not coupled with a concomitant increase in hepatic NEFA. This increase in hepatic lipids was paralleled by a significant increase in plasma triglycerides and VLDL (Table 1). These effects of OLZ were also accompanied by liver injury, as indicated by significant elevations of plasma ALT (~2-fold) and AST (~1.5 fold; Table 1).

JPET Fast Forward. Published on August 7, 2013 as DOI: 10.1124/jpet.113.207621
This article has not been copyedited and formatted. The final version may differ from this version.

OLZ modifies hepatic expression of metabolism-regulating genes

Hepatic steatosis is often mediated via direct alterations in the expression of genes key to lipid and carbohydrate metabolism. To further explore the effects of OLZ on hepatic energy metabolism, mRNA expression of genes that are key in regulating the synthesis and catabolism of carbohydrates and lipids was examined by qRT-PCR (Figure 3, panel A). Four weeks of OLZ administration significantly downregulated the expression of a number of genes involved in lipid biosynthesis, including sterol regulatory element-binding protein 1 (*Srebf1*), fatty acid synthase (*Fasn*), and ATP citrate lyase (*Acly*). Similarly, OLZ treatment upregulated expression of glycogen synthase kinase-3β (*Gsk3b*), a protein that suppresses glycogen synthesis. These changes in expression of anabolism-regulating genes were accompanied by a significant (2.5-fold) increase in expression of glucokinase (*Gck*), a key rate-limiting enzyme in glycolysis. Expression of carnitine palmitoyltransferase 1a (*Cpt1a*), which encodes the rate-limiting enzyme in fatty acid β-oxidation, was unchanged, as were phosphoenolpyruvate carboxykinase 1 (*Pck1*; gluconeogenesis) and glucose transporter type 1 and glucose transporter type 4 (*Glut1* and *Glut4*; basal and insulin-mediated glucose transport, respectively).

Effects of OLZ on mitochondrial respiration

The mRNA expression data suggest that OLZ administration favors glycolysis (Figure 3). Previous studies with isolated brain mitochondria have suggested that OLZ partially inhibits mitochondrial respiration [e.g., (Hroudova and Fisar, 2010)]. The effect of OLZ exposure on the balance between glycolysis and mitochondrial respiration was therefore determined in vitro in HepG2 cells by Seahorse in both glucose- and galactose-containing media (see Materials and Methods). Under these conditions, PPR is used as an index of glycolysis, and the OCR is used as an index of mitochondrial function (Figure 3, panels B and C). As expected, inhibition of mitochondrial respiration with oligomycin, which forced the cells to rely on anaerobic glycolysis,

decreased the rate of OCR, while simultaneously increasing the rate of PPR, thereby greatly increasing the PPR:OCR ratio. Uncoupling the mitochondria with FCCP increased the OCR while still maintaining an elevated PPR, causing the PPR:OCR ratio to decrease relative to oligomycin, but still remain elevated relative to basal (panel B). In glucose-containing medium, OLZ had no apparent effect on OCR or PPR at any concentration. When the Warburg/Crabtree effect was overcome by incubating HepG2 cells in galactose-containing media (Warburg, et al., 1967), the ratio of PPR:OCR was dramatically decreased, as the cells were forced to rely on oxidative phosphorylation (Marroquin, et al., 2007). Under these conditions, OLZ incubation caused a dose-dependent increase in PPR, without significantly affecting OCR; these effects of OLZ significantly increased the PPR:OCR ratio (panels B and C).

Effects of OLZ and glucose and glycogen expenditure

OLZ increased basal (unfasted) plasma glucose, as indicated by plasma taken at sacrifice (Table 1). Previous studies have indicated that OLZ administration may cause insulin resistance and/or glucose intolerance (Coccurello and Moles, 2010). To determine if OLZ administration under the current conditions affected glucose tolerance, fasted mice were subjected to the OGTT at 25 days of vehicle or drug administration (see Materials and Methods; Figure 4, panel A). OLZ did not affect the area-under-the-curve of the OGTT during the testing period. However, OLZ exposure significantly increased plasma glucose concentrations 15 minutes after bolus gavage (panel A), but values were similar to controls at all subsequent time points. As mentioned above, the expression of a key inhibitor of glycogen storage (*Gsk3b*) was significantly increased in livers of OLZ-exposed mice (see Figure 3, panel A). The effect of OLZ administration on hepatic glycogen storage was therefore assessed by periodic acid-Schiff (PAS) staining (Figure 4, panel B, representative photomicrographs, and panel C, quantitative image analysis). OLZ administration significantly decreased the amount of glycogen stores in unfasted liver by 2-fold compared to controls.

OLZ effects on the hepatic metabolome, mTOR and AMPK

Examining metabolites on an individual basis is time-consuming, and the smaller amounts of data produced may unnecessarily narrow the scope of a study. Metabolomic analysis was therefore used to simultaneously characterize several effects of OLZ on liver. Metabolites that varied significantly between the OLZ group and the control group were then analyzed with pathway analysis software, which predicted and mapped the pathways that may be relevant to OLZ treatment (Figure 5, panels A and B). Among other findings, amino acids were significantly affected by OLZ: L-glutamine, a putative mediator of mTOR activation (Nicklin, et al., 2009), was increased in animals administered OLZ. OLZ also caused a decrease in L-leucine and a parallel increase in L-glutamate, which can act as nitrogen donor and nitrogen acceptor, respectively, in the transamination reaction that regulates the glutamate-glutamine cycle (Islam, et al., 2010). Network analysis further predicted the involvement of amino acid transporters Slc7a5 (LAT1) and Slc38a2 (SNAT2), which were recently shown to function as regulators of mTOR signaling, and EAAT3, which is regulated by mTOR activation (Almilaji, et al., 2012).

Given the key role of mTOR in mediating carbohydrate and lipid metabolism, (Tsang, et al., 2007) and the effects of OLZ on these pathways (see Figures 3-5), the effect of OLZ administration on the activation of mTOR and dependent signaling cascades was determined by Western blot (Figure 6). OLZ administration increased mTOR activation, as indicated by a significant increase in phosphorylation at Ser248. OLZ administration also increased phosphorylation of p70S6K at Thr389 and 4EBP1 at Thr37/46, indicative of mTORC1 activation (Hara, et al., 1997), as well as Akt phosphorylation at Ser473, indicative of mTORC2 activation (Guertin, et al., 2006). Interestingly, OLZ treatment also concomitantly increased AMPK activation, as indicated by an increase in phosphorylation at Thr172.

JPET Fast Forward. Published on August 7, 2013 as DOI: 10.1124/jpet.113.207621
This article has not been copyedited and formatted. The final version may differ from this version.

DISCUSSION

As mentioned in the Introduction, OLZ is an effective drug for treating several psychiatric illnesses and is the drug of choice for schizophrenia and bipolar disorder. The benefits of OLZ are countered by side effects such as weight gain, glucose intolerance and dyslipidemia which impact not only treatment compliance but also increase the health risks to patients. An improved understanding of OLZ actions in the peripheral tissue may therefore identify new approaches to increase the long-term safety and utility of this drug.

As has been observed previously, OLZ administration increased body weight and adiposity in mice (Figure 1). Interestingly, this effect of OLZ was not concurrent with a detectable increase in food consumption (Figure 1), which suggests that OLZ administration may directly alter energy usage in vivo. In support of this hypothesis, previous experiments have shown that both acute and chronic OLZ administration dysregulates peripheral carbohydrate and lipid metabolism (Chintoh, et al., 2008;Coccurello and Moles, 2010;Girault, et al., 2012) and directly increases the expression of lipid biosynthetic genes in both liver and adipose tissue (Skrede, et al., 2012). In the current study, OLZ administration caused a complex phenotypic alteration in hepatic carbohydrate metabolism. OLZ administration increased glycolysis without an apparent increase in mitochondrial respiration (Figures 3 and 4) and favored glycogen depletion (Figures 4 and 6).

OLZ administration also caused a slight, but significant, increase in glucose intolerance (Figure 4) and unfasted plasma glucose (Table 1). A shift to an elevated but incomplete (i.e., anaerobic) glycolysis would favor ATP generation from alternate sources, such as lipid oxidation. In support of this hypothesis, OLZ administration increases plasma lactic acid levels in humans (Glavina, et al., 2011), indicative of increased anaerobic glycolysis. Furthermore, OLZ administration lowers the respiratory exchange ratio (RER) in rats (Albaugh, et al., 2012),

indicative of a preferential shift to NEFA over carbohydrates as fuel. These results are in line with the observation here that hepatic and plasma triglycerides were elevated by OLZ administration, without a commensurate increase in NEFA (Figure 2 and Table 1).

Within the cell, carbohydrate and lipid metabolism are usually under tight control by the protein kinases AMPK and mTOR. Both AMPK and mTOR are known to act as "sensors" of cellular energy status and help to maintain homeostasis (Hardie, 2008;Guertin and Sabatini, 2009). In general, the downstream effects of AMPK activation are considered catabolic and favor ATP generation during energy depletion. Glycolysis, for example, is enhanced by AMPK. Signaling downstream of AMPK also inhibits ATP-consuming processes (Krause, et al., 2002). In contrast to AMPK, mTOR is activated during times of high nutrient availability and favors storage of excess nutrients (e.g., as triglycerides). Activation of the mTOR pathway promotes ATP-consuming processes such as protein and lipid synthesis through its downstream targets p70S6K and 4EBP1. Previous studies have demonstrated that AMPK is activated in the CNS by OLZ administration (Kim, et al., 2007). Furthermore, OLZ increases p70S6K1 and 4EBP1 phosphorylation in cultured hepatocytes, indicative of mTOR activation (Oh, et al., 2011). The experiments here demonstrate, for the first time, that OLZ in vivo concomitantly activates AMPK and mTOR pathways in the liver. AMPK and mTOR are generally differentially activated, and mediate opposing cellular functions (Kimball, 2006). The outcomes of OLZ administration on hepatic metabolism may reflect these contradictory inputs. These data suggest that treatment with OLZ results in a pseudo-fasted state wherein metabolic resources are abundant, but cannot be efficiently used.

The reason for OLZ's concurrent activation of AMPK and mTOR is not immediately clear. Should OLZ indeed induce a pseudo-fasted state, the activation of AMPK may be, in principle, via the 'energy sensing' activation of this pathway. As mentioned above, OLZ increases

peripheral concentrations of glutamate and its metabolites [Figure 5; (Goff, et al., 2002;Yudkoff, et al., 2005)]. The increase in these molecules in the liver may directly activate mTOR (Tato, et al., 2011;Laplante and Sabatini, 2012). Previous studies have indicated that activating AMPK with metformin (a classical approach to treat metabolic syndrome) confers a disappointingly small beneficial effect against some of the metabolic effects of OLZ (Ehret, et al., 2010). This lack of effectiveness may be due to the fact that OLZ administration itself activates AMPK. Alternatively, it has been suggested that 'normalizing' mTOR overactivation may be beneficial in obesity and diabetes (Laplante and Sabatini, 2012). It may be that such an approach would be more effective in the context of OLZ administration. The glutamatergic model of mental illness proposes that psychotic disorders are disorders of excitatory amino acid metabolism (Tsai and Coyle, 2002). Therefore, inhibiting mTOR would be arguably 'downstream' of the assumed therapeutic mechanisms of OLZ in psychiatric disorders, and may be a beneficial treatment approach to prevent this drug's metabolic side effects OLZ.

Another important aspect of this work is that OLZ administration significantly increased plasma indices of liver injury in mice (Table 1). Elevation of liver enzymes is described as a common reaction with OLZ administration, and generally results in drug discontinuation (Dominguez-Jimenez, et al., 2012). The pathologic changes observed in liver here (Figure 2) are analogous to those caused by non-alcoholic fatty liver disease (NAFLD). As mentioned in the introduction, obesity and its sequelae (e.g., NAFLD) are reaching alarmingly high levels in developed countries. NAFLD is a spectrum of liver diseases, ranging from the relatively benign simple steatosis, to active inflammation, to advanced fibrosis and cirrhosis, and ultimately hepatocellular carcinoma (Ratziu, et al., 2002). Although the prevalence of simple steatosis in individuals at risk for NAFLD can be very high (i.e., >90%), the prevalence of the more severe stages of the disease is much lower (Machado, et al., 2006). These factors emphasize that the risk for developing more severe stages of NAFLD is not based solely on obesity and other

primary risk factors, but is rather mitigated by other factors or 'hits' (Day and James, 1998). It is therefore possible that the metabolic effects of OLZ administration could serve as such a second 'hit' in NAFLD.

JPET Fast Forward. Published on August 7, 2013 as DOI: 10.1124/jpet.113.207621
This article has not been copyedited and formatted. The final version may differ from this version.

Authorship Contributions

Participated in research design: Robin H. Schmidt, Xiang Zhang and Gavin E. Arteel

Conducted experiments: Robin H. Schmidt, Jenny D. Jokinen, Veronica L. Massey, K. Cameron Falkner, Xue Shi, Xinmin Yin, Juliane I. Beier,

Contributed new reagents or analytical tools. Xiang Zhang

Performed data analysis. Robin H. Schmidt, Xiang Zhang, Xue Shi, Xinmin Yin, Juliane I. Beier and Gavin E. Arteel

Wrote or contributed to the writing of the manuscript: Robin H. Schmidt, Xue Shi, Xiang Zhang and Gavin E. Arteel

Reference List

Albaugh VL, Vary TC, Ilkayeva O, Wenner BR, Maresca KP, Joyal JL, Breazeale S, Elich TD, Lang CH and Lynch CJ (2012) Atypical antipsychotics rapidly and inappropriately switch peripheral fuel utilization to lipids, impairing metabolic flexibility in rodents. *Schizophr Bull* **38**:153-166.

Allison DB, Newcomer JW, Dunn AL, Blumenthal JA, Fabricatore AN, Daumit GL, Cope MB, Riley WT, Vreeland B, Hibbeln JR and Alpert JE (2009) Obesity Among Those with Mental Disorders: A National Institute of Mental Health Meeting Report. *Am J Prev Med* **36**:341-350.

Almilaji A, Pakladok T, Guo A, Munoz C, Foller M and Lang F (2012) Regulation of the glutamate transporter EAAT3 by mammalian target of rapamycin mTOR. *Biochem Biophys Res Commun* **421**:159-163.

Andrikopoulos S, Blair AR, Deluca N, Fam BC and Proietto J (2008) Evaluating the glucose tolerance test in mice. *Am J Physiol Endocrinol Metab* **295**:E1323-E1332.

Bergheim I, Guo L, Davis MA, Lambert JC, Beier JI, Duveau I, Luyendyk JP, Roth RA and Arteel GE (2006) Metformin prevents alcohol-induced liver injury in the mouse: Critical role of plasminogen activator inhibitor-1. *Gastroenterology* **130**:2099-2112.

Bligh EG and Dyer WJ (1959) A rapid method of total lipid extraction and purification. *Can J Biochem Physiol* **37**:911-917.

Chintoh AF, Mann SW, Lam L, Lam C, Cohn TA, Fletcher PJ, Nobrega JN, Giacca A and Remington G (2008) Insulin resistance and decreased glucose-stimulated insulin secretion after acute olanzapine administration. *J Clin Psychopharmacol* **28**:494-499.

Coccurello R and Moles A (2010) Potential mechanisms of atypical antipsychotic-induced metabolic derangement: Clues for understanding obesity and novel drug design. *Pharmacol Therapeut* **127**:210-251.

Cope MB, Nagy TR, Fernandez JR, Geary N, Casey DE and Allison DB (2005) Antipsychotic drug-induced weight gain: development of an animal model. *Int J Obes* **29**:607-614.

Day CP and James OF (1998) Steatohepatitis: a tale of two "hits"? *Gastroenterology* **114**:842-845.

Dominguez-Jimenez JL, Puente-Gutierrez JJ, Pelado-Garcia EM, Cuesta-Cubillas D and Garcia-Moreno AM (2012) Liver toxicity due to olanzapine. *Rev Esp Enferm Dig* **104**:617-618.

Ehret M, Goethe J, Lanosa M and Coleman CI (2010) The effect of metformin on anthropometrics and insulin resistance in patients receiving atypical antipsychotic agents: a meta-analysis. *J Clin Psychiatry* **71**:1286-1292.

Girault EM, Alkemade A, Foppen E, Ackermans MT, Fliers E and Kalsbeek A (2012) Acute peripheral but not central administration of olanzapine induces hyperglycemia associated with hepatic and extra-hepatic insulin resistance. *PLoS One* **7**:e43244.

Glavina T, Mrass D, Dodig T, Glavina G, Pranic S and Uglesic B (2011) Blood lactate levels in patients receiving first- or second- generation antipsychotics. *Croat Med J* **52**:41-47.

Goff DC, Hennen J, Lyoo IK, Tsai G, Wald LL, Evins AE, Yurgelun-Todd DA and Renshaw PF (2002) Modulation of brain and serum glutamatergic concentrations following a switch from conventional neuroleptics to olanzapine. *Biol Psychiatry* **51**:493-497.

Grayson BE, Seeley RJ and Sandoval DA (2013) Wired on sugar: the role of the CNS in the regulation of glucose homeostasis. *Nat Rev Neurosci* **14**:24-37.

Guertin DA and Sabatini DM (2009) The pharmacology of mTOR inhibition. *Sci Signal* **2**:e24.

Guertin DA, Stevens DM, Thoreen CC, Burds AA, Kalaany NY, Moffat J, Brown M, Fitzgerald KJ and Sabatini DM (2006) Ablation in mice of the mTORC components raptor, rictor, or mLST8 reveals that mTORC2 is required for signaling to Akt-FOXO and PKCalpha, but not S6K1. *Dev Cell* **11**:859-871.

Hara H, Yonezawa K, Kozlowski MT, Sugimoto T, Andrabi K, Weng QP, Kasuga M, Nishimoto I and Avruch J (1997) Regulation of eIF-4E BP1 phosphorylation by mTOR. *J Biol Chem* **272**:26457-26463.

Hardie DG (2008) AMP-activated/SNF1 protein kinases: conserved guardians of cellular energy. *Nat Rev Mol Cell Biol* **8**:774-785.

Heiskanen T, Niskanen L, Lyytikainen R, Saarinen PI and Hintikka J (2003) Metabolic syndrome in patients with schizophrenia. *J Clin Psychiatry* **64**:575-579.

Hroudova J and Fisar Z (2010) Activities of respiratory chain complexes and citrate synthase influenced by pharmacologically different antidepressants and mood stabilizers. *Neuroendocrinology Letters* **31**:336-342.

Islam MM, Nautiyal M, Wynn RM, Mobley JA, Chuang DT and Hutson SM (2010) Branched-chain amino acid metabolon: interaction of glutamate dehydrogenase with the mitochondrial branched-chain aminotransferase (BCATm). *J Biol Chem* **285**:265-276.

Kapur S, VanderSpek SC, Brownlee BA and Nobrega JN (2003) Antipsychotic dosing in preclinical models is often unrepresentative of the clinical condition: a suggested solution based on in vivo occupancy. *J Pharmacol Exp Ther* **305**:625-631.

Kim SF, Huang AS, Snowman AM, Teuscher C and Snyder SH (2007) Antipsychotic drug-induced weight gain mediated by histamine H1 receptor-linked activation of hypothalamic AMP-kinase. *Proc Natl Acad Sci U S A* **104**:3456-3459.

Kimball SR (2006) Interaction between the AMPK-Activated Protein Kinase and mTOR Signaling Pathways. *Med Sci Sports Exerc* **38**:1958-1964.

Krause U, Bertrand L and Hue L (2002) Control of p70 ribosomal protein S6 kinase and acetyl-CoA carboxylase by AMP-activated protein kinase and protein phosphatases in isolated hepatocytes. *Eur J Biochem* **269**:3751-3759.

Laplante M and Sabatini DM (2012) mTOR signaling in growth control and disease. *Cell* **149**:274-293.

Lee CT, Conde BJ, Mazlan M, Visanuyothin T, Wang A, Wong MM, Walker DJ, Roychowdhury SM, Wang H and Tran PV (2002) Switching to Olanzapine From Previous Antipsychotics: A Regional Collaborative Multicenter Trial Assessing 2 Switching Techniques in Asia Pacific. *J Clin Psychiatry* **63**:569-576.

Machado M, Marques-Vidal P and Cortez-Pinto H (2006) Hepatic histology in obese patients undergoing bariatric surgery. *J Hepatol* **45**:600-606.

Maher AR and Theodore G (2012) Summary of the comparative effectiveness review on off-label use of atypical antipsychotics. *J Manag Care Pharm* **18**:S1-S20.

Marroquin LD, Hynes J, Dykens JA, Jamieson JD and Will Y (2007) Circumventing the Crabtree Effect: Replacing Media Glucose with Galactose Increases Susceptibility of HepG2 Cells to Mitochondrial Toxicants. *Tox Sci* **97**:539-547.

Mathews M and Muzina DJ (2007) Atypical antipsychotics: new drugs, new challenges. *Cleve Clin J Med* **74**:597-606.

Nicklin P, Bergman P, Zhang B, Triantafellow E, Wang H, Nyfeler B, Yang H, Hild M, Kung C, Wilson C, Myer VE, MacKeigan JP, Porter JA, Wang YK, Cantley LC, Finan PM and Murphy LO (2009) Bidirectional transport of amino acids regulates mTOR and autophagy. *Cell* **136**:521-534.

Ogden CL, Carroll MD, Curtin LR, McDowell MA, Tabak CJ and Flegal KM (2006) Prevalence of overweight and obesity in the United States, 1999-2004. *JAMA* **295**:1549-1555.

Oh KJ, Park J, Lee SY, Hwang I, Kim JB, Park TS, Lee HJ and Koo SH (2011) Atypical antipsychotic drugs perturb AMPK-dependent regulation of hepatic lipid metabolism. *Am J Physiol Endocrinol Metab* **300**:E624-E632.

Ratziu V, Bonyhay L, Di M, V, Charlotte F, Cavallaro L, Sayegh-Tainturier MH, Giral P, Grimaldi A, Opolon P and Poynard T (2002) Survival, liver failure, and hepatocellular carcinoma in obesity-related cryptogenic cirrhosis. *Hepatology* **35**:1485-1493.

Sandoval DA, Obici S and Seeley RJ (2009) Targeting the CNS to treat type 2 diabetes. *Nat Rev Drug Discov* **8**:386-398.

Skrede S, Ferno J, Vazquez MJ, Fjaer S, Pavlin T, Lunder N, Vidal-Puig A, Dieguez C, Berge RK, Lopez M and Steen VM (2012) Olanzapine, but not aripiprazole, weight-independently elevates serum triglycerides and activates lipogenic gene expression in female rats. *Int J Neuropsychopharmacol* **15**:163-179.

Tato I, Bartrons R, Ventura F and Rosa JL (2011) Amino acids activate mammalian target of rapamycin complex 2 (mTORC2) via PI3K/Akt signaling. *J Biol Chem* **286**:6128-6142.

Tsai G and Coyle JT (2002) Glutamatergic mechanisms in schizophrenia. *Annu Rev Pharmacol Toxicol* **42:165-79.**:165-179.

Tsang CK, Qi H, Liu LF and Zheng XF (2007) Targeting mammalian target of rapamycin (mTOR) for health and diseases. *Drug Discov Today* **12**:112-124.

van der Zwaal EM, Luijendijk MCM, Adan RAH and la Fleur SE (2008) Olanzapine-induced weight gain: Chronic infusion using osmotic minipumps does not result in stable plasma levels due to degradation of olanzapine in solution. *Eur J Pharmacol* **585**:130-136.

Warburg O, Geissler AW and Lorenz S (1967) Uber Wachstum von Krebszellen in Medien, deren Glucose durch Galaktose ersetzt ist. *Hoppe Seylers Z Physiol Chem* **348**:1686-1687.

Wei X, Shi X, Koo I, Kim S, Schmidt RH, Arteel GE, Watson WH, McClain C and Zhang X (2013) MetPP: a computational platform for comprehensive two-dimensional gas chromatography time-of-flight mass spectrometry-based metabolomics. *Bioinformatics*.

Weiden PJ, Mackell JA and McDonnell DD (2004) Obesity as a risk factor for antipsychotic noncompliance. *Schizophr Res* **66**:51-57.

Weston-Green K, Huang XF and Deng C (2012) Alterations to Melanocortinergic, GABAergic and Cannabinoid Neurotransmission Associated with Olanzapine-Induced Weight Gain. *PLoS One* **7**:e33548.

Yudkoff M, Daikhin Y, Nissim I, Horyn O, Luhovyy B, Lazarow A and Nissim I (2005) Brain amino acid requirements and toxicity: the example of leucine. *J Nutr* **135**:1531S-1538S.

Zhang J, Fang A, Wang B, Kim SH, Bogdanov B, Zhou Z, McClain C and Zhang X (2011) iMatch: a retention index tool for analysis of gas chromatography-mass spectrometry data. *J Chromatogr A* **1218**:6522-6530.

Footnotes

*This work supported by National Institutes of Health National Institute of General Medical Sciences (GM087735); RHS and VLM were supported by a predoctoral (T32) fellowship from National Institutes of Health National Institute of Environmental Health Science (ES011564).

JPET Fast Forward. Published on August 7, 2013 as DOI: 10.1124/jpet.113.207621
This article has not been copyedited and formatted. The final version may differ from this version.

Figure legends

Figure 1: Effect of OLZ on body weight gain and adiposity

Panel A shows a schematic of the experimental design. Average weekly food consumption and weight gain (panel B) and fat pad and total body fat (panel C) were determined as described in Materials and Methods. Panel D depicts representative DEXA Scan images. Low density areas depict soft matter (i.e., body fat). *$p < 0.05$ compared to controls.

Figure 2: OLZ promotes hepatic lipid accumulation

Panel A shows representative photomicrographs depicting general histology (H&E; upper panels) and lipid accumulation (Oil Red O; lower panels). Hepatic triglyceride (TG) and non-esterified fatty acid (NEFA) contents were as described in Materials and Methods (panel B). Liver weight measurements taken at sacrifice are expressed as a percentage of total body weight (panel C). *$p < 0.05$ compared to controls.

Figure 3: Effects of OLZ on hepatic expression of metabolism-regulating genes and in vitro metabolism of OLZ-treated HepG2 cells

Hepatic mRNA expression of genes for lipid and carbohydrate metabolism was determined by qRT-PCR (panel A), as described in Materials and Methods. Panel B shows OCR and PPR rate data (Seahorse) for all time points in HepG2 cells treated with 25 uM OLZ or control as described in Materials and Methods. The effect of increasing concentrations of OLZ on steady-state PPR:OCR are depicted in panel C. *$p < 0.05$ compared to controls.

Figure 4: Effects of OLZ and glucose and glycogen expenditure

The effect of OLZ on oral glucose tolerance (OGTT) was assessed as described in Materials and Methods (panel A). Panel B depicts representative photomicrographs stained for glycogen

content (PAS), while panel C summarizes quantitative image-analysis of PAS staining. *p < 0.05 compared to controls by repeated measures ANOVA (panel A) or t-test (panel C).

Figure 5: OLZ effects on hepatic metabolite profile

Metabolites were determined by GC×GC-TOF MS and evaluated with MetaCore™ software and used to construct a pathway map (panel A), as described in Materials and Methods. Abundance data is shown for selected metabolites (panel B). *, p < .05 compared to controls.

Figure 6: OLZ mediates signaling through mTOR pathways

Liver homogenates were prepared as described in Materials and Methods. Representative Immunoblots are shown (panel A). Quantitative analysis was performed and the ratio of phosphorylated to total protein is shown in (panel B). Proposed mechanisms by which OLZ administration activates mTOR (panel C). OLZ promotes flux of glutamine (Gln) and leucine (Leu) through solute carrier 38a2 (SLC38A2 or SNAT2) and solute carrier 7a5 (SLC7A5 or LAT1). Increased concentrations of Gln and Leu induce mTOR signaling. Excess intracellular Leu acts as a nitrogen donor in the branched chain aminotransferase (BCAT) reaction that forms glutamate (Glu). Leu and Glu also contribute metabolic intermediates (e.g., acetyl CoA) to the Krebs cycle. Interestingly, AMPK was simultaneously activated under these conditions (see discussion for additional information). *p < 0.05 compared to controls.

JPET Fast Forward. Published on August 7, 2013 as DOI: 10.1124/jpet.113.207621
This article has not been copyedited and formatted. The final version may differ from this version.

Table 1.

		Control	OLZ
Glucose	(mg/dL)	196 ± 6	329 ± 13*
Trig.	(mg/dL)	42 ± 2	80 ± 7*
Cholesterol	(mg/dL)	50 ± 6	62 ± 3
HDL	(mg/dL)	34 ± 4	42 ± 4
LDL	(mg/dL)	8 ± 2	4 ± 2
VLDL	(mg/dL)	9 ± 1	16 ± 1*
ALT	(U/L)	33 ± 9	76 ± 9*
AST	(U/L)	56 ± 2	80 ± 6*

Animals and treatments are described in Materials and Methods. Data are means ±S.E.M. (n=4-8) and are reported as indicated in the individual rows. *, $P < .05$ compared to controls.

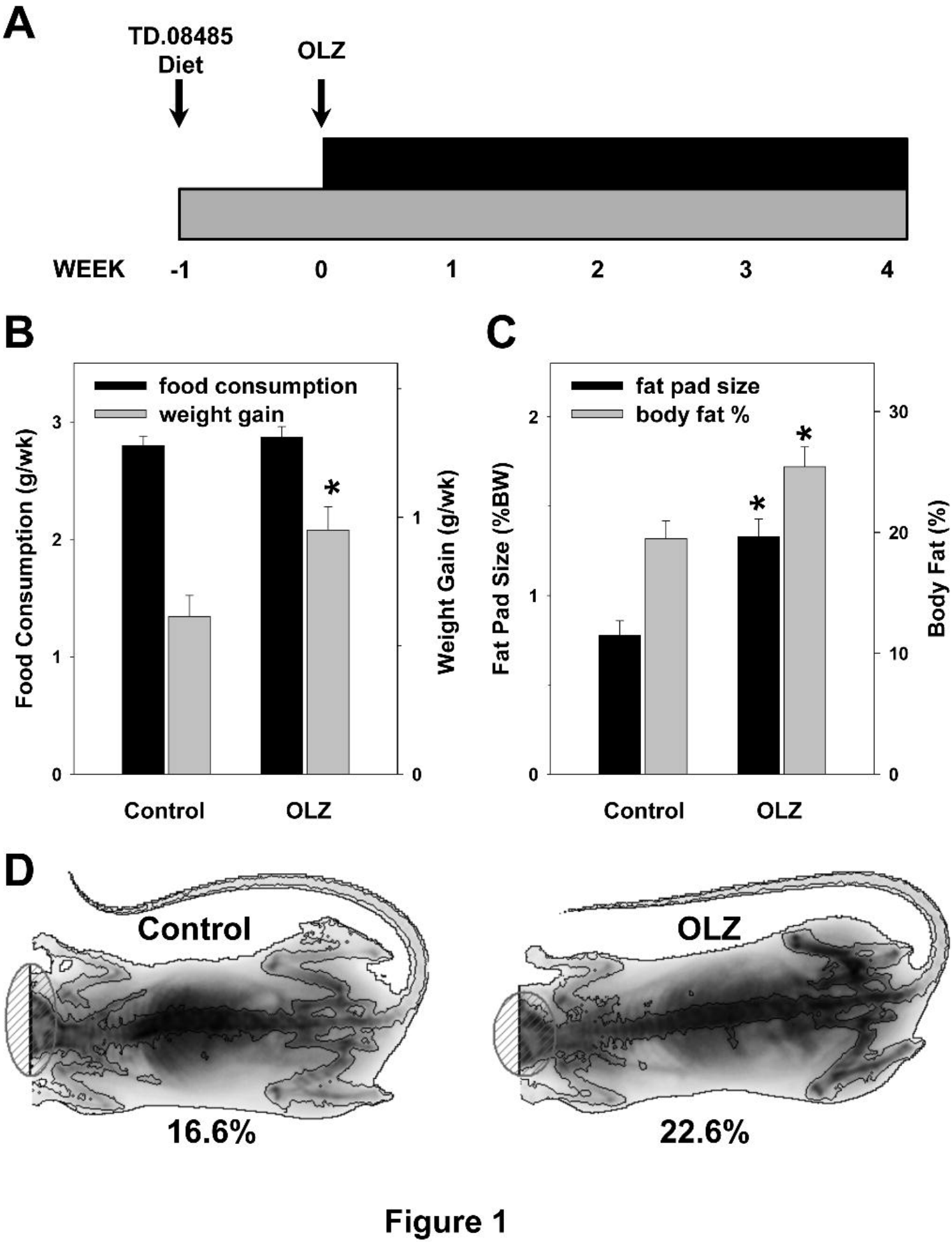
A
TD.08485
Diet
OLZ
WEEK
-1
0
1
2
3
4
B
food consumption
weight gain
Food Consumption (g/wk)
Weight Gain (g/wk)
Control
OLZ
C
fat pad size
body fat %
Fat Pad Size (%BW)
Body Fat (%)
Control
OLZ
D
Control
16.6%
OLZ
22.6%

Figure 1

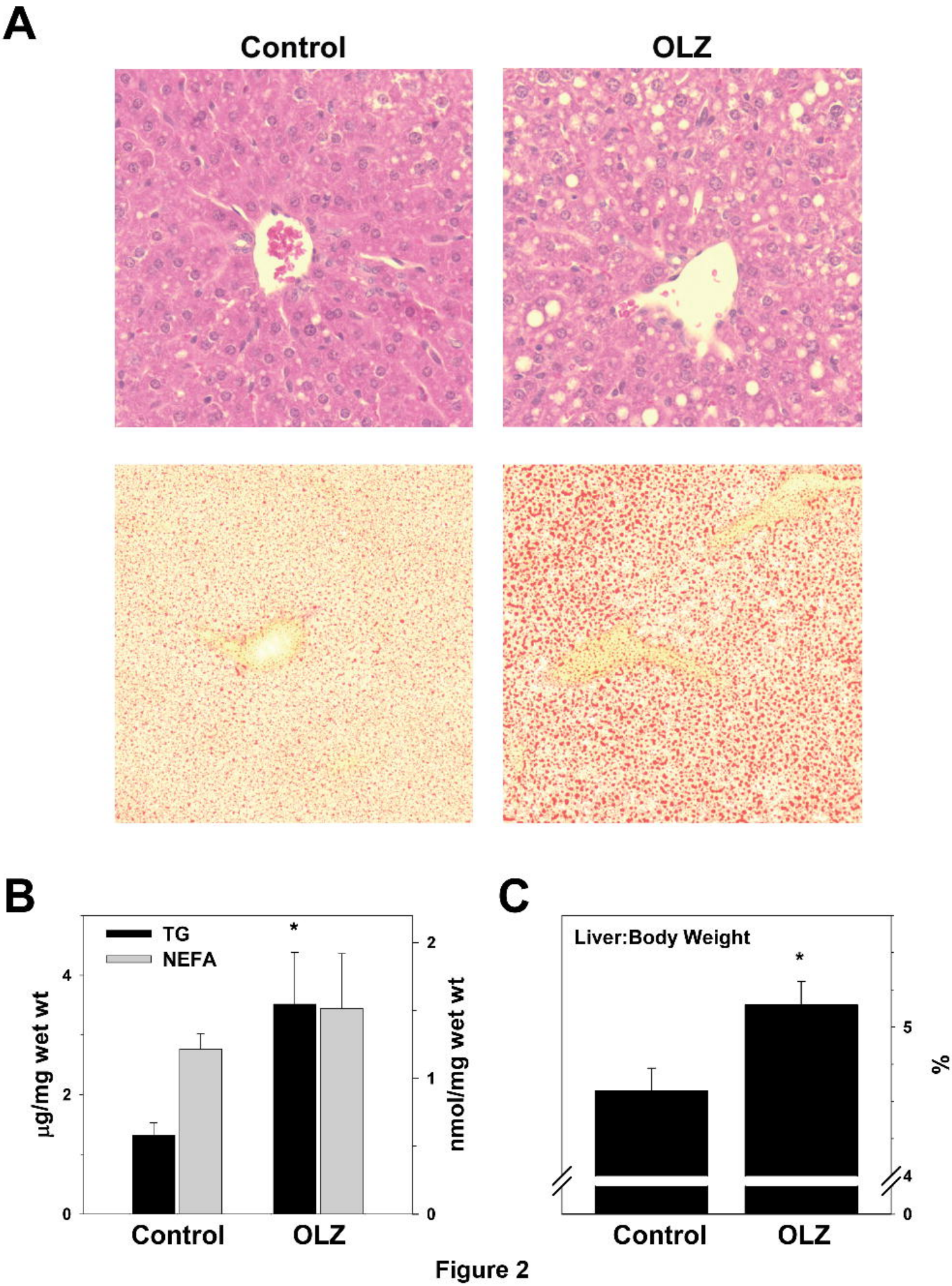
A
Control
OLZ
B
TG
NEFA
*
μg/mg wet wt
nmol/mg wet wt
0
2
4
0
1
2
Control
OLZ
C
Liver:Body Weight
*
%
0
4
5
Control
OLZ

Figure 2

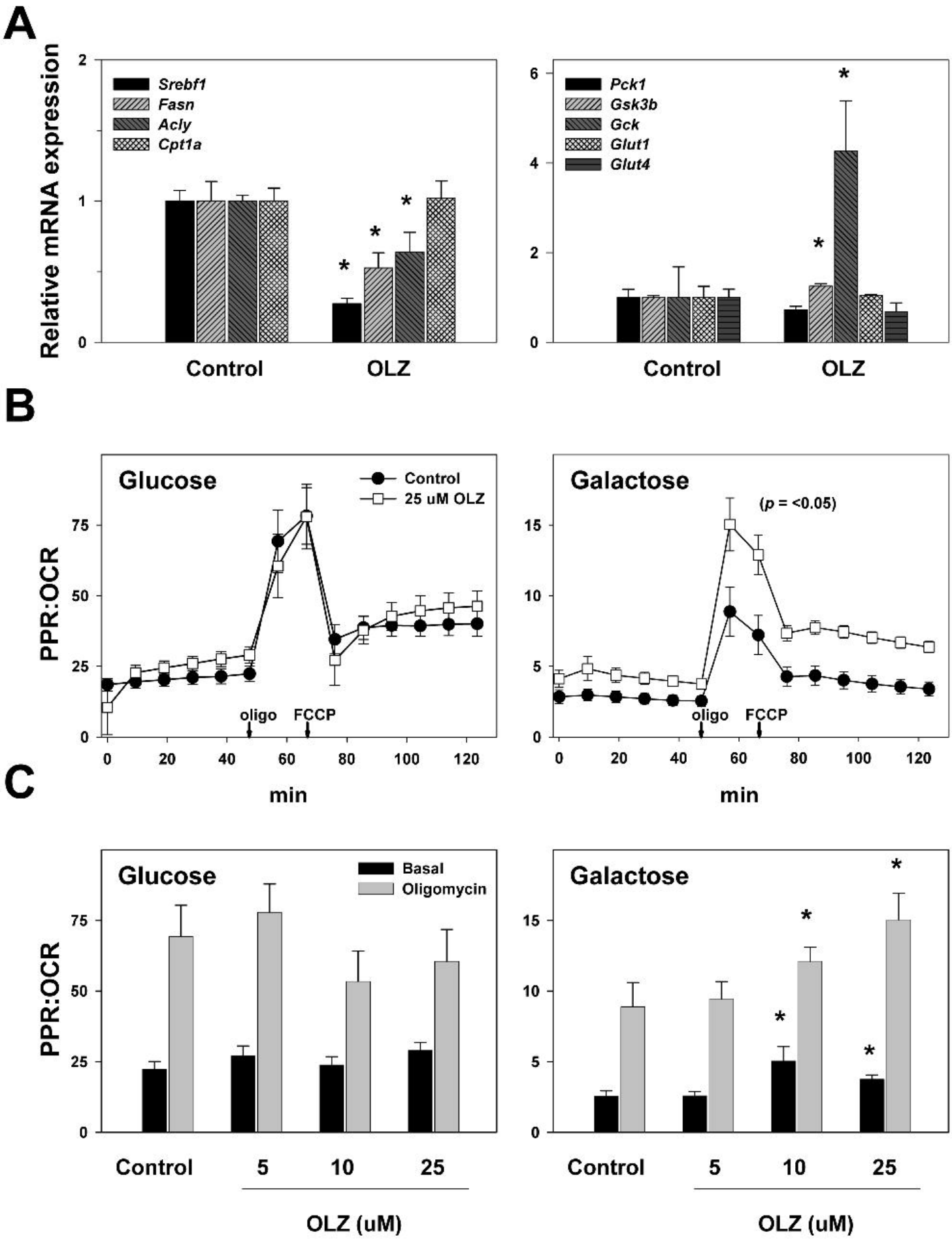
A
Relative mRNA expression
Srebf1
Fasn
Acly
Cpt1a
Control
OLZ
Pck1
Gsk3b
Gck
Glut1
Glut4
Control
OLZ
B
PPR:OCR
Glucose
Control
25 uM OLZ
oligo
FCCP
min
Galactose
(p = <0.05)
oligo
FCCP
min
C
PPR:OCR
Glucose
Basal
Oligomycin
Control
5
10
25
OLZ (uM)
Galactose
Control
5
10
25
OLZ (uM)

Figure 3

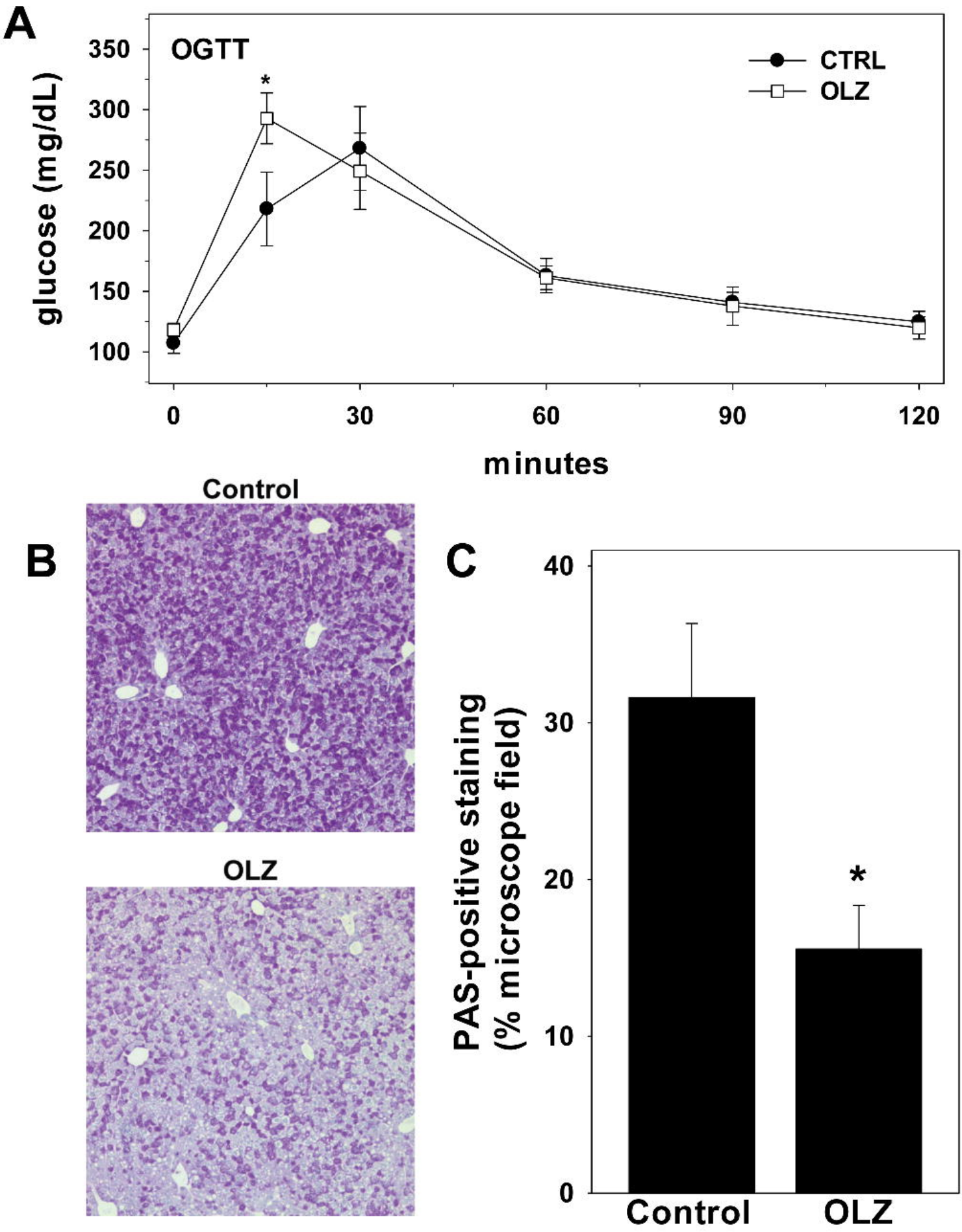
A
OGTT
CTRL
OLZ
glucose (mg/dL)
350
300
250
200
150
100
*
0
30
60
90
120
minutes
B
Control
OLZ
C
PAS-positive staining
(% microscope field)
40
30
20
10
0
*
Control
OLZ

Figure 4

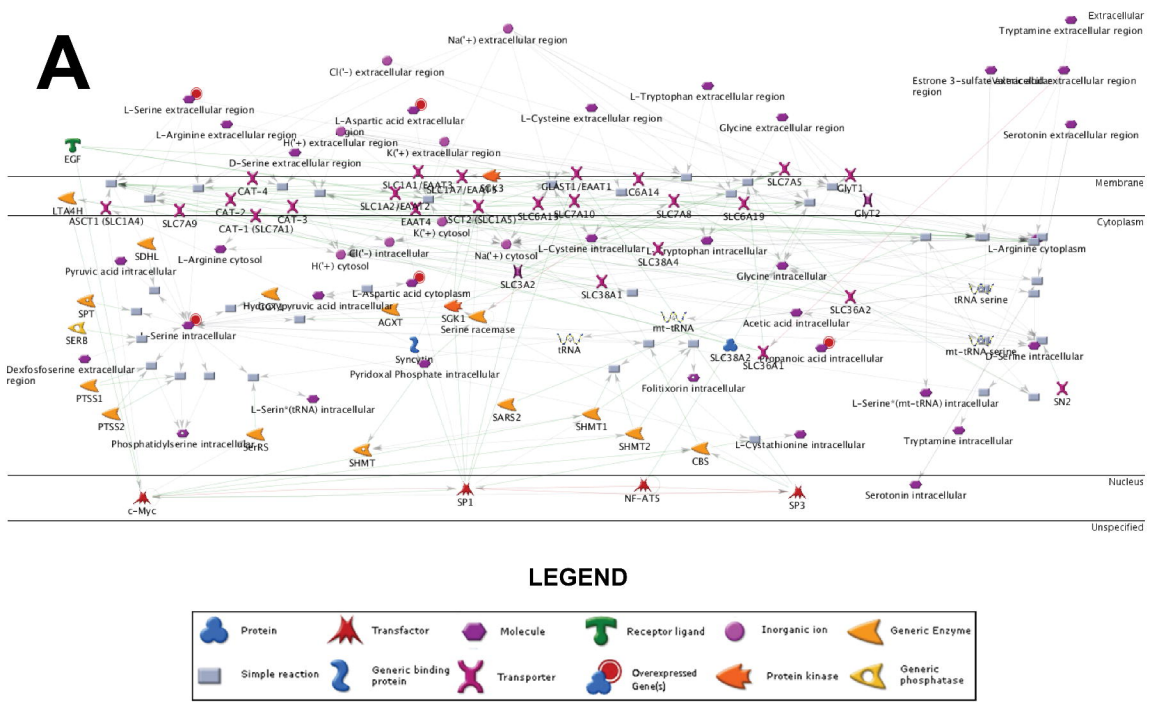

LEGEND

B

OLZ compared to CONTROL

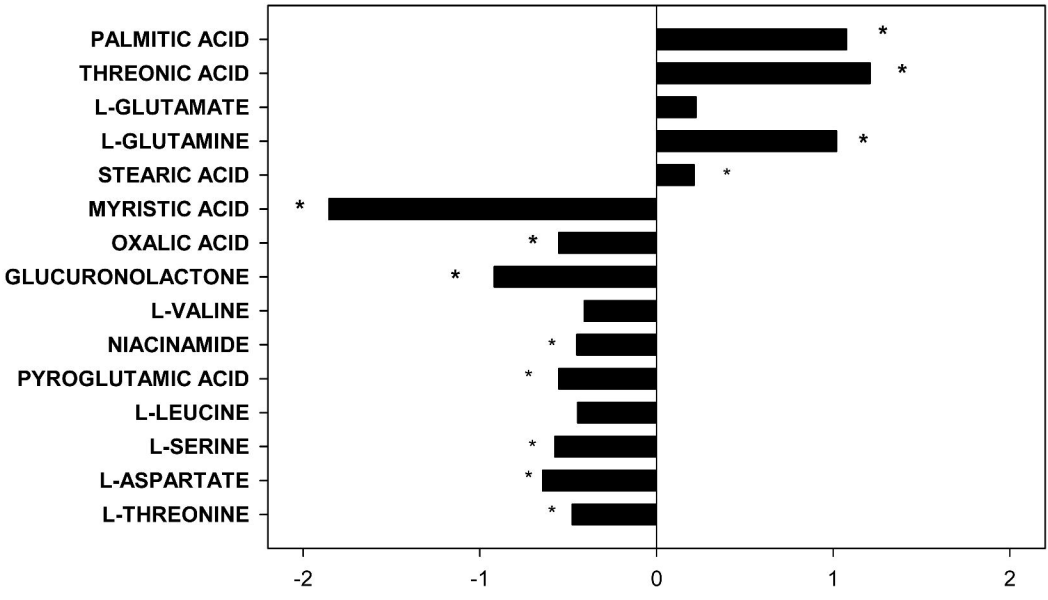

Figure 5

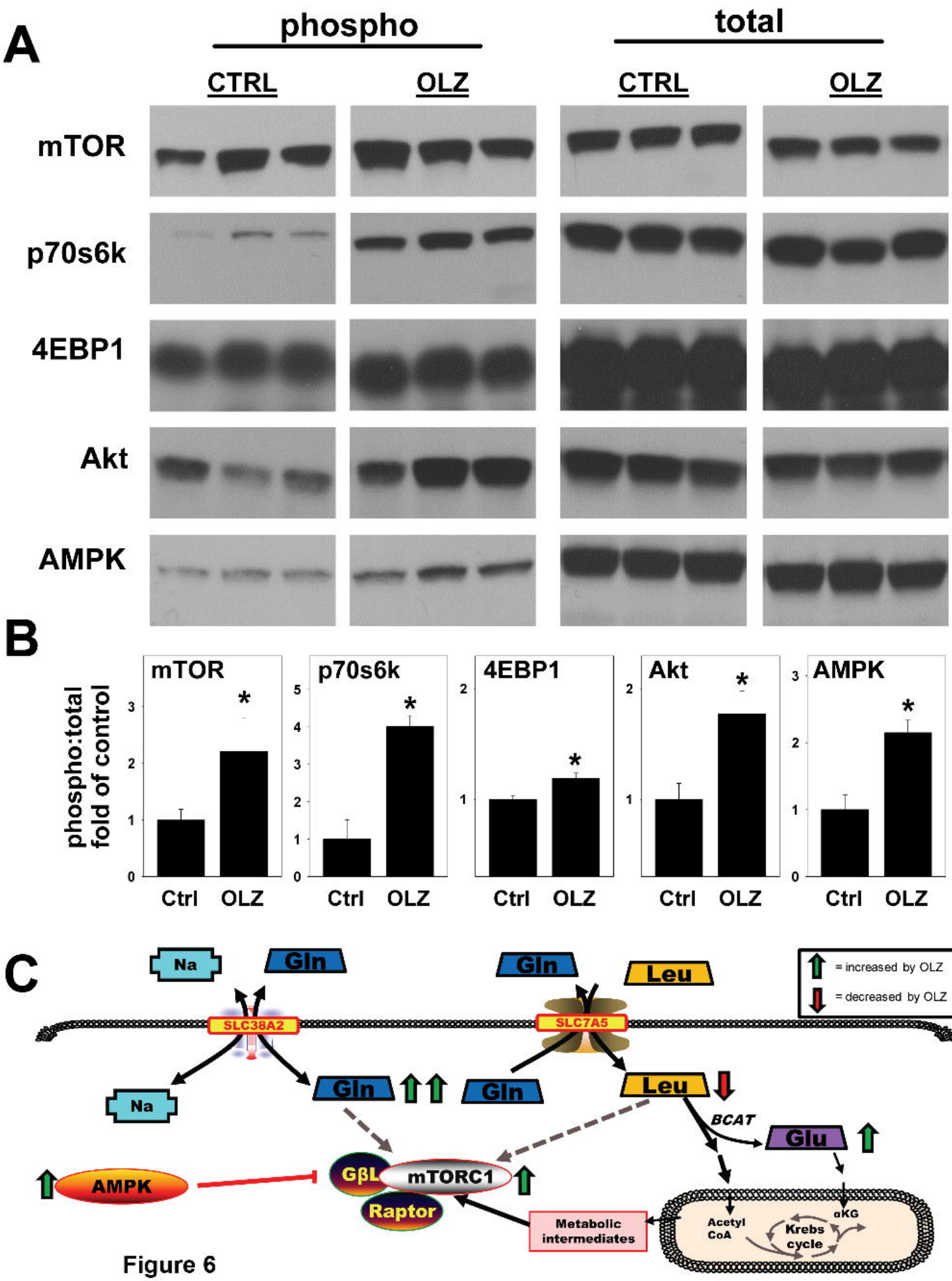
A
phospho
total
CTRL
OLZ
CTRL
OLZ
mTOR
p70s6k
4EBP1
Akt
AMPK
B
phospho:total
fold of control
mTOR
p70s6k
4EBP1
Akt
AMPK
Ctrl
OLZ
C
Na
Gln
Gln
Leu
= increased by OLZ
= decreased by OLZ
SLC38A2
SLC7A5
Na
Gln
Gln
Leu
BCAT
Glu
AMPK
GβL
mTORC1
Raptor
Metabolic intermediates
Acetyl CoA
Krebs cycle
αKG

Figure 6